Higher-Order Basis Functions Applied to the Inverse Method of Moments for Inverse-Source Problems

O. Borries[1,2], E. Jørgensen[1], P. Meincke[1], and P. C. Hansen[2]

[1]: TICRA, Læderstræde 34, DK-1201 København K, Denmark, ob@ticra.com, ej@ticra.com, pme@ticra.com
[2]: Department of Informatics and Mathematical Modelling, Technical University of Denmark, Building 321, DK-2800 Lyngby, Denmark, pch@imm.dtu.dk

Abstract

Higher-order basis functions are commonly used for discretization of surface integral equations, which are typically solved by the Method of Moments (MoM). This leads to higher accuracy and lower memory requirements when compared to a simple piecewise linear discretization, e.g., RWG functions. Typical applications of these techniques are antenna or scattering problems where the excitation is known and the radiated or scattered fields are desired. The present paper investigates the use of higher-order basis functions when applied to the Inverse MoM where the radiated field has been measured and the electromagnetic sources producing the radiated field are the unknown quantities. The typical applications of this method are antenna diagnostics and filtering of measured fields.

Keywords: Inverse Method of Moments, antenna diagnostics, source reconstruction, higher-order basis functions

1 Introduction

Antenna diagnostics have traditionally been performed by using FFT-based back-propagation to a planar aperture. Full 3D reconstruction of equivalent currents on a surface enclosing the antenna has been investigated by several research groups in the last decade [1]–[6]. Here, the reconstruction problem can be formulated as an inverse-source problem involving a set of integral equations, which may be discretized using a standard MoM-discretization. This leads to a (possibly over-determined) system of linear equations that is not trivial to solve due to the inevitable measurement noise and the ill-posed nature of the problem. However, for the case of first-order basis functions it was shown in [3]–[6] that the problem can be solved by taking advantage of the inherently regularizing property of a conjugate-gradient style solver.

An improved Inverse MoM for 3D source reconstruction was introduced recently [7], [8]. This new technique employs smooth curvilinear geometry modeling and higher-order hierarchical Legendre basis functions of arbitrary order [9], in conjunction with a robust iterative solution scheme. While higher-order basis functions have been successfully applied in numerous works employing the forward MoM, it is not obvious that the high polynomial order will be beneficial in the Inverse MoM. To this end, this paper investigates the effect of employing higher-order basis functions in the Inverse MoM by considering a simple case using synthetic data with and without added noise. In particular, we demonstrate that the high polynomial expansion order has a favorable impact on the convergence rate of the iterative solution scheme as well as on the reconstruction error that can be achieved. The proposed higher-order Inverse MoM has been applied to practical antenna diagnostics problems in [8], [10].

2 Formulation of the Inverse Problem

The inverse source problem was presented in [7] and a brief summary is given below. On the reconstruction surface S enclosing an antenna, the equivalent electric and magnetic surface current densities are defined as

$$\mathbf{J}_S = \hat{\mathbf{n}} \times \mathbf{H} \tag{1a}$$

$$\mathbf{M}_S = -\hat{\mathbf{n}} \times \mathbf{E}, \tag{1b}$$

where $\mathbf{E}$ and $\mathbf{H}$ are the fields just outside the surface of reconstruction. In addition to satisfying (1), these equivalent currents satisfy Love's equivalence principle, i.e., they produce a zero field inside S.

The measured field at a point $\mathbf{r}$ outside S can now be written as

$$\mathbf{E}^{\text{meas}}(\mathbf{r}) = -\eta_0 \mathcal{L} \mathbf{J}_S + \mathcal{K} \mathbf{M}_S, \tag{2}$$

where η_0 is the free-space impedance and the integral operators $\mathcal{L}$ and $\mathcal{K}$ are defined by

$$\mathcal{L}\mathbf{J}_S = j\omega\mu_0 \left[\int_S \mathbf{J}_S(\mathbf{r}')G(\mathbf{r},\mathbf{r}')\,dS' + \frac{1}{k_0^2}\int_S \nabla_S' \cdot \mathbf{J}_S(\mathbf{r}')\nabla G(\mathbf{r},\mathbf{r}')\,dS' \right] \tag{3a}$$

$$\mathcal{K}\mathbf{M}_S = \int_S \mathbf{M}_S(\mathbf{r}') \times \nabla G(\mathbf{r},\mathbf{r}')\,dS', \tag{3b}$$

where k_0 is the free-space wavenumber and $G(\mathbf{r},\mathbf{r}')$ is the scalar Green's function of free space. Equation (2) is referred to as the data equation, since it relates the measured data $\mathbf{E}^{\text{meas}}$ and the unknown surface current densities $\mathbf{J}_S$ and $\mathbf{M}_S$.

The formulation based on (2) and (3) is ambiguous; to obtain the desired unique physical current densities in (1) we must ensure that the field radiated by these currents is zero inside S, cf. [2], [6]. This leads to the following equations which must hold for $\mathbf{r} \in S$:

$$-\eta_0 \hat{\mathbf{n}} \times \mathcal{L}\mathbf{J}_S + \left(\hat{\mathbf{n}} \times \mathcal{K} + \frac{1}{2} \right) \mathbf{M}_S = 0, \tag{4a}$$

$$-\left(\hat{\mathbf{n}} \times \mathcal{K} + \frac{1}{2} \right) \mathbf{J}_S - \frac{1}{\eta_0} \hat{\mathbf{n}} \times \mathcal{L}\mathbf{M}_S = 0. \tag{4b}$$

These expressions are referred to as the boundary condition equations.

3 Discretization

The surface of reconstruction S is discretized using curvilinear patches of up to fourth order. Let (u,v) denote the coordinates on a path; then the electric and magnetic surface currents on each patch are expanded as

$$\mathbf{X}_S = \sum_{m=0}^{M^u} \sum_{n=0}^{M^v-1} a_{mn}^u \mathbf{B}_{mn}^u + \sum_{m=0}^{M^v} \sum_{n=0}^{M^u-1} a_{mn}^v \mathbf{B}_{mn}^v \tag{5}$$

where $\mathbf{X}_S = [\mathbf{J}_S, \mathbf{M}_S]$, a_{mn}^u and a_{mn}^v are the expansion coefficients, M^u and M^v are expansion orders along the u- and v-directions, and $\mathbf{B}_{mn}^u$ and $\mathbf{B}_{mn}^v$ are the Legendre basis functions in the u and v directions [9] defined as

$$\mathbf{B}_{mn}^u(u,v) = \frac{\mathbf{a}_u}{\mathcal{J}_s(u,v)}\widetilde{P}_m(u)\,P_n(v)\,, \quad \mathbf{B}_{mn}^v(u,v) = \frac{\mathbf{a}_v}{\mathcal{J}_s(u,v)}\widetilde{P}_m(v)\,P_n(u)\,. \tag{6}$$

Here, $\mathbf{a}_u$ and $\mathbf{a}_v$ are the covariant unitary vectors and $\mathcal{J}_s(u,v) = |\mathbf{a}_u \times \mathbf{a}_v|$ is the surface Jacobian.

To obtain the desired linear systems of equations, the above current expansion is inserted in the data equation (2) and the boundary condition equation (4). The coefficient matrix $\mathbf{A}$ corresponding to the data equation is obtained by evaluating the $\hat{\theta}$ and $\hat{\phi}$ components of $\mathbf{E}^{\text{meas}}$ at each measurement sampling point. The elements of the

coefficient matrix $\mathbf{L}$ corresponding to the boundary conditions are obtained by means of a quasi-Galerkin testing scheme using contravariant unitary vectors [7, (8)]. This readily leads to the coupled equations

$$\mathbf{Ax} \approx \mathbf{b} \qquad \text{and} \qquad \mathbf{Lx} = \mathbf{0}, \tag{7}$$

where $\mathbf{x}$ is a vector of unknown basis function coefficients, $\mathbf{b}$ contains samples of the measured field, $\mathbf{A}$ is an $M \times N$ matrix with elements representing the field radiated by a particular basis function observed at the measurement points, and $\mathbf{L}$ is a $P \times N$ matrix whose elements are the inner products of the field on the surface radiated by a particular basis function, and a particular testing function on S (these test functions are identical to the basis functions for the field). The matrix $\mathbf{L}$ is typically chosen to be square, i.e., $P = N$.

4 Solving the Linear Equations

In order to compute an accurate solution we must balance the effects of noise with the requirement of achieving Love's currents. Hence, we express the discretized model in (7) as a general-form discrete Tikhonov problem

$$\min_{\mathbf{x}} \left\{ \|\mathbf{Ax} - \mathbf{b}\|_2^2 + \alpha^2 \|\mathbf{Lx}\|_2^2 \right\}, \tag{8}$$

in which the regularization parameter α works as the balancing factor – as the noise-level increases, α can be increased to put more emphasis on achieving Love's currents, thereby controlling the solution. Selecting α automatically is done using the L-curve criterion, discussed in [11, §5].

We note that the formulation (8) is equivalent to a least squares problem

$$\min_{\mathbf{x}} \left\| \begin{bmatrix} \mathbf{A} \\ \mathbf{L} \end{bmatrix} \mathbf{x} - \begin{bmatrix} \mathbf{b} \\ \mathbf{0} \end{bmatrix} \right\|_2, \tag{9}$$

which can be solved by standard iterative methods such as conjugate gradients [2, 5, 6]. However, the relative balancing (or scaling) of the matrices $\mathbf{A}$ and $\mathbf{L}$ in (9) is a non-trivial matter, and hence the stacked-matrix approach may lack the robustness needed to perform well across a range of cases and noise levels.

In order to achieve a more robust and general approach, we use an algorithm based on the inherent regularizing properties of the conjugate gradient method – using the fact that the projection onto the relevant Krylov subspace underlying the method has a regularizing effect (known as semi-convergence), see [11, §6]. Hence, in this approach the number of iterations plays the role of the regularization parameter. In order to incorporate the matrix $\mathbf{L}$ into the iterative approach, we use this matrix as a right preconditioner as described in [11, §8], has the effect of ensuring that the computed solution satisfies (8). Again, we can use the L-curve criterion to determine the optimal number of iterations.

5 Numerical Experiments

To investigate the performance of the higher-order basis functions when used in antenna diagnostics, we will use a simple synthetic test case: A spherical reconstruction surface S with radius 0.3λ and 5 dipoles placed inside the sphere, as shown in Table 1. The far-field radiated by these dipoles is used to generate the measured field.

Position (x, y, z) [λ]	Orientation (θ, ϕ) [deg]	Excitation [A]	Type
$(0,0,0)$	$(20,40)$	$1\angle 0°$	Electric
$(-0.1,0,0)$	$(-10,0)$	$1\angle 30°$	Magnetic
$(0.1,0,0)$	$(45,30)$	$1\angle 0°$	Electric
$(0,0.1,0)$	$(90,0)$	$1\angle 0°$	Electric
$(0,-0.1,0)$	$(90,0)$	$1\angle 0°$	Magnetic

Table 1: Position, orientation, excitation, and type of the five dipoles used for the test case behind Figure 1.

Figure 1 shows the RMS errors averaged for the electric and magnetic fields. For reference, the relative root mean square error RMS_E between the reconstructed and exact electric fields, $\mathbf{E}_{\text{rec}}$ and $\mathbf{E}_{\text{exact}}$, is determined by

$$\text{RMS}_E = \sqrt{\frac{\int_S |\hat{\mathbf{n}} \times \mathbf{E}_{\text{rec}} - \hat{\mathbf{n}} \times \mathbf{E}_{\text{exact}}|^2 \, dS}{\int_S |\hat{\mathbf{n}} \times \mathbf{E}_{\text{exact}}|^2 \, dS}}, \tag{10}$$

and RMS_H is calculated similarly. The RMS is plotted against the iteration number for our preconditioned conjugate gradient scheme, both for a noise-free setting and for a setting where the signal-to-noise ratio (SNR) is 60 dB. The noise is modeled as uncorrelated Gaussian noise which is added to the real and imaginary parts of the calculated fields before performing the reconstruction. As an alternative to the higher-order scheme, we also present results obtained with first-order (piecewise linear) basis functions and the iterative approach employed in [6].

Figure 1 demonstrates the superior accuracy of the higher-order approach when coupled with an efficient iterative solver. The RMS is significantly lower than the first-order implementation when comparing solutions with the same number of unknowns. Hence, the low-order solution requires substantially more memory and a substantially higher iteration count to achieve a given accuracy. Comparing the optimal solutions achieved by the higher-order and first-order approaches, we note that there is an order of magnitude improvement for the noise-free setting, while the RMS of the higher-order solution is approximately half that of the lower-order solution in the case of 60 dB SNR. Furthermore, it is interesting to note the strong similarity between the behavior for the first-order approach when comparing the noise-free and SNR = 60 dB cases. This suggests that the main error bound for that approach is the discretization error.

An important aspect to address in the Inverse MoM is the stopping criterion for the iterative method. For the higher-order implementation this is particularly important, since (due to the semi-convergence) the solution deteriorates after a certain point, which reflects the ill-posedness of the underlying continuous problem. A fully automated and robust stopping criterion based on the L-curve has been implemented, and this criterion allows the algorithm to be stopped when the optimal accuracy has been achieved.

6 Conclusion

The accuracy of the higher-order Inverse MoM has been investigated and compared to the commonly used first-order algorithm. Numerical results obtained for synthetic measurements demonstrate that the higher-order approach yields far more accurate solutions and requires less memory than the first-order approach. The algorithm presented here is a powerful tool for antenna diagnostics and for processing of measured fields, e.g., artificial removal of undesired contributions from cables and mounting structures. Examples demonstrating these new capabilities will be shown at the symposium.
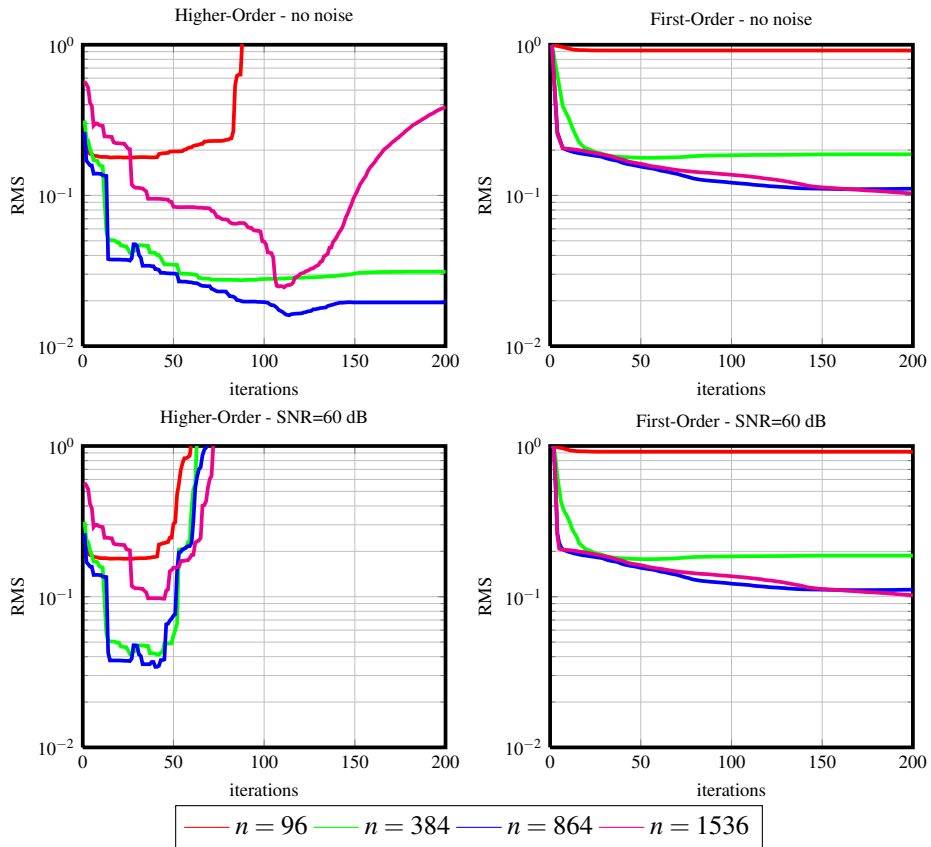
Figure 1: RMS errors. Left: Higher-Order solution, increasing the number of unknowns by increasing the order - 4th order yields $n = 1536$. Right: First-Order solution, increasing the number of unknowns by decreasing the meshsize. We note that increasing the number of iterates for the first-order cases does not improve the results. Using even finer discretization meshes for the first-order method, yielding $n = 3456$ and $n = 8664$ unknowns, provides slightly better accuracy, around 8% RMS.

References

[1] T. K. Sarkar and A. Taaghol, "Near-field to near/far-field transformation for arbitrary near-field geometry utilizing and equivalent electric current and MoM", IEEE Trans. Antennas Propagat., vol. 47, no. 3, pp. 566–573, Mar. 1999.

[2] K. Persson and M. Gustafsson, "Reconstruction of equivalent currents using a near-field data transformation - with radome applications", Progress in Electromagnetics Research, vol. 54, pp. 179–198, 2005.

[3] Y. Alvarez, F. Las-Heras, M. R. Pino, and J. A. Lopez, "Acceleration of the sources reconstruction method via the fast multipole technique", in "IEEE Antennas and Propagation Society International Symposium", San Diego, CA, USA, July 2008.

[4] T. F. Eibert and C. H. Schmidt, "Multilevel fast multipole accelerated inverse equivalent current method employing rao-wilton-glisson discretization of electric and magnetic surface currents", IEEE Trans. on Antennas Propagat., vol. 57, no. 4, pp. 1178–1185, 2009.

[5] J. L. A. Quijano and G. Vecchi, "Improved-accuracy source reconstruction on arbitrary 3-D surfaces", IEEE Antennas and Wireless Propagation Letters, vol. 8, pp. 1046–1049, 2009.

[6] J. L. A. Quijano and G. Vecchi, "Field and source equivalence in source reconstruction on 3D surfaces", Progress in Electromagnetics Research, vol. PIER-103, pp. 67–100, 2010.

[7] E. Jørgensen, P. Meincke, C. Cappellin, and M. Sabbadini, "Improved source reconstruction technique for antenna diagnostics", Proceedings of the 32nd ESA Antenna Workshop, ESTEC, Noordwijk, The Netherlands, 2010.

[8] E. Jørgensen, P. Meincke, O. Borries, and M. Sabbadini, "Processing of measured fields using advanced inverse method of moments algorithm", Proceedings of the 33rd ESA Antenna Workshop, ESTEC, Noordwijk, The Netherlands, 2011.

[9] E. Jørgensen, J. L. Volakis, P. Meincke, and O. Breinbjerg, "Higher order hierarchical Legendre basis functions for electromagnetic modeling", IEEE Trans. Antennas and Propagat., vol. 52, no. 11, pp. 2985–2995, Nov. 2004.

[10] E. Jørgensen, P. Meincke, and C. Cappellin, "Advanced processing of measured fields using field reconstruction techniques", Proceedings of European Conference on Antennas and Propagation, EuCAP, Rome, Italy, 2011.

[11] P. C. Hansen, "Discrete Inverse Problems – Insight and Algorithms", SIAM, Philadelphia, PA, 2010.